Design and Characterization of an $Al_xGa_{1-x}As/Ga_xIn_{1-x}As_yP_{1-y}$ Multijunction Solar Cell

A Dissertation
Submitted in Partial Fulfillment of the Requirement for the Degree of
Bachelor of Science in Electrical and Electronic Engineering

Submitted by

Abdullah Bin Shams

Shadman Nafis

Mohammad Zawad Ali

Under the supervision of

Dr. Md. Ashraful Hoque
Professor
Department of Electrical and Electronic Engineering
Islamic University of Technology (IUT)
Organization of Islamic Cooperation (OIC)
Board Bazar, Gazipur-1704
Bangladesh

Design and Characterization of an $Al_xGa_{1-x}As/Ga_xIn_{1-x}As_yP_{1-y}$ Multijunction Solar Cell

A thesis presented to

The academic faculty

By

Abdullah Bin Shams (Student ID: 092422)

Shadman Nafis (Student ID: 092418)

Mohammad Zawad Ali (Student ID: 092438)

In Partial Fulfillment of Requirement for the Degree of

Bachelor of Science in Electrical and Electronic Engineering

Approved by

Dr. Md. Ashraful Hoque

Professor

Department of Electrical and Electronic Engineering

Islamic University of Technology (IUT)

Organization of Islamic Cooperation (OIC)

October, 2013

A Dissertation on

Design and Characterization of an $Al_xGa_{1-x}As/Ga_xIn_{1-x}As_yP_{1-y}$ Multijunction Solar Cell

Submitted by

_____   _____   _____

Abdullah Bin Shams   Shadman Nafis   Mohammad Zawad Ali
(ID: 092422)   (ID: 092418)   (ID: 092438)

Approved by

_____

Dr. Md. Shahid Ullah
Professor and Head
Department of EEE
Islamic University of Technology (IUT)

_____

Dr. Md. Ashraful Hoque (Thesis supervisor)
Professor
Department of EEE
Islamic University of Technology (IUT)

Acknowledgements

Abstract

Unlike general solar cell modeling with AlGaAs in this work $Al_xGa_{1-x}As/Ga_xIn_{1-x}As_yP_{1-y}$ Multijunction Solar Cell was designed with Ge substrate. Several parameters were then calculated using AMPS-1D and wxAMPS simulation software i.e. Efficiency, Fill Factor, Open circuit voltage (V_{oc}) and Short circuit current density (J_{sc}) to characterize this solar cell model. It was also shown that a higher bandgap difference between the n and p type materials of the tunnel junction produced a higher efficiency for this design and finally the tunnel junction was optimized. As an extension of this design from two junctions to three and four Junctions, appropriate designs were also proposed using GaAsSb and GaInAs.

Table of Contents

List of Figures

List of Tables

Symbols & Abbreviations

I   Current (A)

I_L Photocurrent (A)

I_F Forward current (A)

I_s Saturation current (A)

k   Boltzmann constant (1.38×10^{-23} JK^{-1})

T   Absolute temperature (K)

e   Charge of an electron (C)

I_{sc} Short-circuit current (A)

V_{oc} Open-circuit voltage (V)

P_m Maximum output power (W)

V_m Voltage at maximum power point (V)

I_m Current at maximum power point (A)

FF   Fill Factor

η   Energy conversion efficiency (%)

E   Solar irradiance (W/cm^2)

A   Area of the solar cell (cm^2)

J_{sc} Short-circuit current density (A/cm^2)

ξ   Electric field (V/m)

Eg   Band energy (eV)

h   Plank's constant (6.63×10^{-34} Js)

c   Speed of light (3×10^8 m/s)

α   Absorption coefficient (m^{-1})

λ   Wavelength (m)

AM   Air Mass

Chapter 1- Introduction

1.1   Alternate Energy

While a majority of the world's current electricity supply is generated from fossil fuels such as coal, oil and natural gas, these traditional energy sources face a number of challenges including rising prices, security concerns over dependence on imports from a limited number of countries which have significant fossil fuel supplies, and growing environmental concerns over the climate change risks associated with power generation using fossil fuels. As a result of these and other challenges facing traditional energy sources, governments, businesses and consumers are increasingly supporting the development of alternative energy sources and new technologies for electricity generation. Renewable energy sources such as solar, biomass, geothermal, hydroelectric and wind power generation have emerged as potential alternatives which address some of these concerns. As opposed to fossil fuels, which draw on finite resources that may eventually become too expensive to retrieve, renewable energy sources are generally unlimited in availability [1].

1.2   Solar Cells

1.2.1   History [2]

The history of photovoltaics dates back to 1839 when the first photovoltaic effect was discovered by Alexandre Becquerel, a 19-year old French experimental physicist. The discovery came as a surprise when Becquerel found a rise in the conductance of metal electrodes under illumination. However, Becquerel's discovery couldn't find any practical use and was limited being tagged as an observed phenomenon. Similar effect was noticed by Willoughby Smith in 1873 while working with Selenium.

Finally in 1883 a working solar cell was constructed by Charles Fritts using selenium on a thin layer of gold which gave an energy efficiency of less than 1%. Though experimented, the theoretical explanation of the photovoltaic effect and the solar cells was not comprehensible till the next century.

In 1932 the photovoltaic effect in Cadmium selenide (a photovoltaic material used till today) was discovered by Audobert and Stora. In 1948 Gordon Teal and John Little constructed single-crystalline germanium and, later, silicon- the ultimate photovoltaic material.

In 1954 the Bell Labs announced the invention of the first modern silicon solar cell with an efficiency index of 6%. However, the high cost of solar photovoltaic electricity was made it impossible to be sustained commercially. In 1957 it cost 1,785$ for 1 watt of photovoltaic energy. So the use was limited to laboratory experiments and space engineering only. The first solar-powered satellite was Vanguard I which ran for eight years. It was a major success in the history of the photovoltaics.

In 1959, Hoffman Electronics introduced commercially available solar cells with 10% efficiency.

In 1955 first sun-powered automobile was demonstrated in Chicago. In 1963, Sharp Corporation developed the first usable photovoltaic module from silicon solar cells. In 1976 the first amorphous (means no original shape or form, non-crystalline) silicon solar cell was developed by RCA Laboratories. By 1977, the world production of photovoltaic modules exceeded 500 kW.

In 1983 Solar Trek vehicle with photovoltaic system of 1 kW drove 4,000 km in twenty days of Australia Race. The maximum speed was 72 km/h, and the average speed was 24 km/h. The same year the vehicle surpassed the distance of 4,000 km between Long Beach, California, and Daytona Beach, Florida, in 18 days.

In 1984, a 1 MW photovoltaic power plant began to operate in Sacramento, California. In 1986, ARCO Solar introduced a G-4000, the first commercial thin film photovoltaic module.

In the Pentax World Solar Challenge 1997 race through Australia a General Motors Sunracer vehicle won with average speed of 71 km/h. On August 13, 2001; after long research and trial, the solar powered plane HELIOS broke the record of high-flying by reaching 30,000 meters.

Today, going beyond science projects and laboratory experiments, the use of photovoltaics has spread all over. Even in under-developed countries, solar projects are being used extensively. At present there are a number of projects with megawatt plus power output. The efficiency of the cell has increased amazingly, too. The new record in solar power efficiency is 42.8% achieved by University of Delaware in July 2007. It's not anymore a distant future when we will have a big share of national power consumptions topped up by the solar energy.

1.2.2   Solar Energy Compared to Other Alternative Energy Sources [3]

Wind is basically created with the temperature changes. We also know that the wind blows from a high pressure area to a low pressure area. These changes in the temperature and pressure occur due to the difference in the amounts of heat energy received by different areas from the sun depending on the earth's rotation. This energy in the form of wind can be converted into electrical or chemical energy, stored in the batteries. The devices used to tap this wind energy are windmills. As the wind blows the rotational energy of turbines is converted into electrical energy by generators. The process is clean, eco-friendly and also renewable.

One wind mill can produce enough energy to power a house. However the electrical energy that is produced from the turbines is not enough compared to the energy produced from the fossil fuels. The disadvantage is that it is costly and not completely renewable; therefore a better way needs to be discovered to produce energy completely clean and eco-friendly. As the wind does not blow at a constant speed and there is no certainty about the wind direction and therefore the output is not efficient as it should be. Also, the wind mills subjected to a severe damage when struck by heavy rains and lightning storms can be subjected to heavy damage. The second is the biomass.

Biomass is a true renewable source of energy. This is because the substance used to produce energy is the excretal waste and remains of plants and animals, also human waste.

Basically any organic material can produce bio energy. This therefore includes agricultural wastes, organic wastes, waste paper and waste from the food processing industries.

Since this type of waste keeps getting produced every day and in tons, there is no chance that the biomass energy such as bio fuel can get exhausted. The cons are similar to the wind power, very expensive therefore not enough energy output. Apart from these constraints, a bi product is created nitrogen oxide which is not good for the atmosphere if produced in large amounts.

Next is the solar energy, out of all the three energy sources this one is the most diversified form of renewable energy. Sun's heat energy can be used for various purposes which make it versatile. Through technological advancement, we have the capability to tap solar energy and produce energy and then store it.

We also have developed devices that can harness the sun's heat energy for different purposes such as distilling water, boiling water for bathing or drinking etc. the cons is that the sunlight only remains for some time during the day and therefore our solar panels should be efficient enough to absorb enough energy that can take us through the day.

But as mentioned above efficient panels have been built and there is hope that we will be able to create solar panels powerful enough to absorb more energy and become self-sufficient. Therefore solar energy seems to be the true alternative energy source we can turn to.

1.2.3   Advantages of Solar Power [4]

Reduced Dependence on Fossil Fuels: Solar energy production does not require fossil fuels and is therefore less dependent on this limited and expensive natural resource. Although there is variability in the amount and timing of sunlight over the day, season and year, a properly sized and configured system can be designed to be highly reliable while providing long-term, fixed price electricity supply.

Environmental Advantages: Solar power production generates electricity with a limited impact on the environment as compared to other forms of electricity production.

Matching Peak Time Output with Peak Time Demand: Solar energy can effectively supplement electricity supply from an electricity transmission grid, such as when electricity demand peaks in the summer

Modularity and Scalability: As the size and generating capacity of a solar system are a function of the number of solar modules installed, applications of solar technology are readily scalable and versatile.

Flexible Locations: Solar power production facilities can be installed at the customer site which reduces required investments in production and transportation infrastructure.

1.2.4 Solar Energy Spectrum
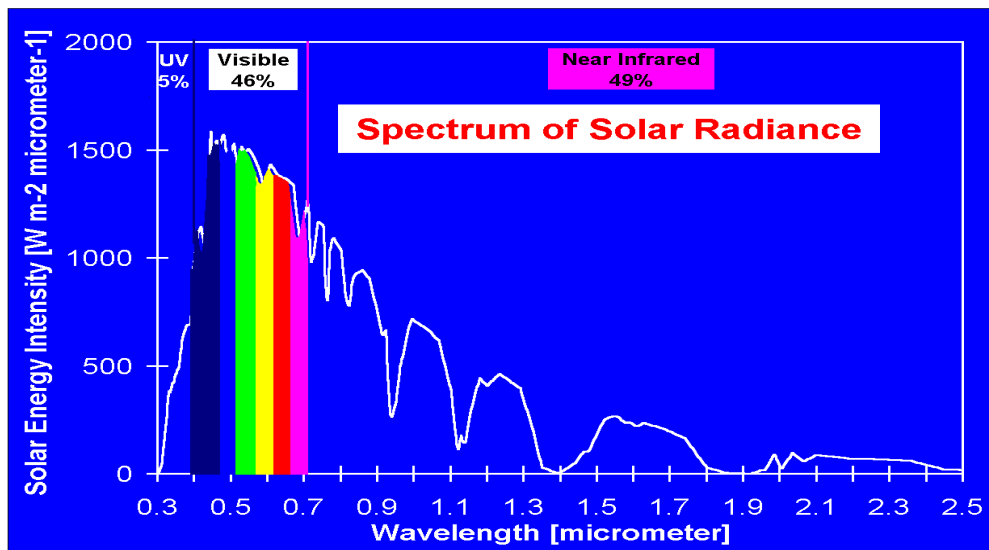
Figure 1.1: Solar energy spectrum

Solar power reaching earth is 1.37 KW/m2. Thus by harnessing this much amount of power we can almost meet all our electrical demand.

1.2.5   Characterization Parameters of a Solar Cell [5]

In order to be able to compare solar modules, standard test conditions have been designed. These conditions include spectrum, intensity and temperature. The standard spectra refer to generic locations. They are prefixed "AM", which stands for "Air Mass" and followed by a number, which refers to the length of the path through the atmosphere in relation to the shortest length if the sun was in the apex.

It is defined by:

$$AM = \frac{1}{\cos(\theta)}$$

where θ is the zenith angle & it is equal to 48° (degree's) which defines the standardized test condition of AM1.5. For AM1.5:-

$$Solar\ radiation = 1000\ W/m^2$$

$$Operating\ temperature = 300\ K$$
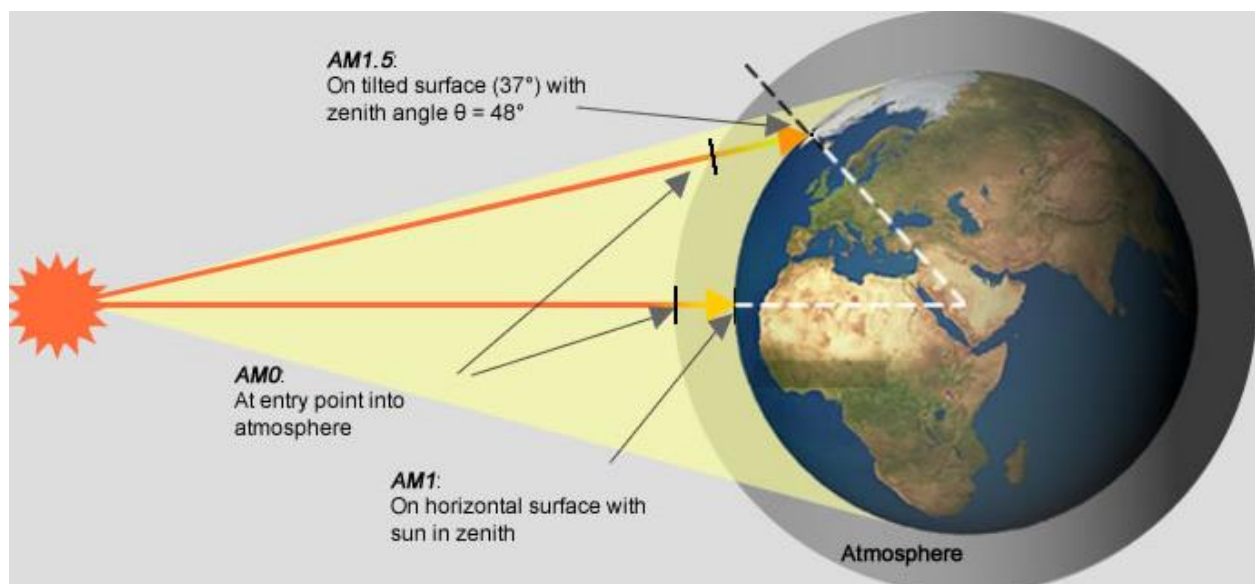
Figure 1.2: Different standard solar spectra

9

1.2.6   Applications of Solar Cells

- Watches.

- Satellites.

- Solar vehicles [6].

- Solar roadways [7].

- Photovoltaic power systems [9].

- Rural electrification [10].

- Calculators [11].

1.2.7   List of Types of Solar Cells [12]

- Quantum Dot Solar Cell.

- Multijunction Solar Cell.

- Plasmonic Solar Cell.

- Organic Solar Cell.

- Thin Film Solar Cell.

1.3   About the Software

1.3.1 AMPS-1D [13]

AMPS-1D (**A**nalysis of **M**icroelectronic and **P**hotonic **S**tructures) software was used for the simulations in this work. It was developed by Professor Stephen J. Fonash and his group from the Pennsylvania State University. AMPS is a very general program for analyzing and designing transport in microelectronic and photonic structures.

It is a 1D simulation tool that simulates device transport by solving the three governing equations: Poisson's equation, the continuity equation for free holes and continuity equation for free electrons with appropriate boundary conditions. AMPS may be used to examine a variety of device structure including multi-junction solar cell structures.

The results of a simulation can be viewed graphically. Light and dark I-V characteristics, electric field, band diagram, carrier density, etc. can be easily plotted. This software requires various material and device parameters such as bandgap, carrier concentration, mobility, doping level, absorption coefficient, layer thickness, etc. as input.

1.3.2 wxAMPS [14]

wxAMPS is a new software designed in UIUC, collaborated with Nankai University of China. It follows the physical principle of AMPS, adds the portion of tunneling currents, improves the convergence property, and provides a better visualization. The software was developed under supervision of Prof. Rockett, Yiming Liu of UIUC.

1.3 Research Outlines

Several studies have been done on $Al_xGa_{1-x}As/GaAs$ single junction solar cells where bandgrading was also implemented to improve its performance [47, 49]. In this work we have proposed & simulated 2 Junction Solar cell using $Al_xGa_{1-x}As$ & $Ga_xIn_{1-x}As_yP_{1-y}$ with Ge as the substrate. Furthermore we have optimized the tunnel junction connecting the two adjacent subcells.

Chapter – 2   Background studies

2.1   Anatomy of a P-N junction [15]

P-N junction & the internal electric field (ξ)**:** Let us consider separate regions of p- and n-type semiconductor material, brought together to form a junction. This is not a practical way of forming a device, but this "thought experiment" does allow us to discover the requirements of equilibrium at a junction. Before they are joined, the n material has a large concentration of electrons and few holes, whereas the converse is true for the p-material. Upon joining the two regions we expect diffusion of carriers to take place because of the large carrier concentration gradients at the junction. Thus holes diffuse from the p-side into the n-side, and electrons diffuse from n to p.

The resulting diffusion current cannot buildup indefinitely, however, because an opposing electric field is created at the junction. If the two regions were boxes of red air molecules and green molecules (perhaps due to appropriate types of pollution), eventually there would be a homogeneous mixture of the two after the boxes were joined. This cannot occur in the case of the charged particles in a p-n junction because of the development of space charge and the electric field (ξ).

If we consider that electrons diffusing from n to p leave behind uncompensated donor ions (N_d^+) in the n material, and holes leaving the p region leave behind uncompensated acceptors (N_a^-), it is easy to visualize the development of a region of positive space charge near the n side of the junction and negative charge near the p side.

The resulting electric field is directed from the positive charge toward the negative charge. Thus ξ is in the direction opposite to that of diffusion current for each type of carrier (recall electron current is opposite to the direction of electron flow).
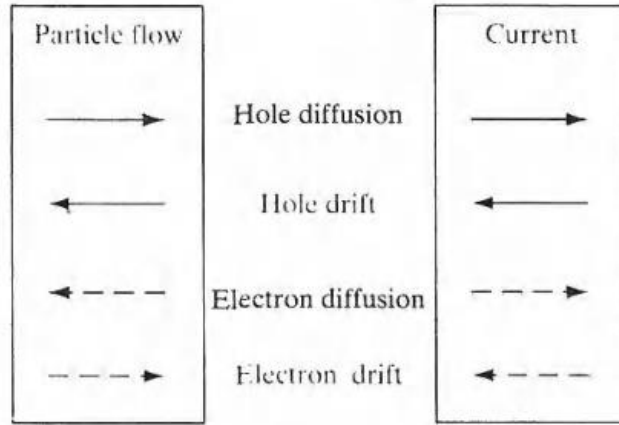
Figure 2.1: Direction for four components of particle flow

and the resulting direction of currents

Therefore, the field creates a drift component of current from n to p, opposing the diffusion current. Since we know that no net current can flow across the junction at equilibrium, the current due to the drift of carriers in the ξ field must exactly cancel the diffusion current. Furthermore, since there can be no net buildup of electrons or holes on either side as a function of time, the drift and diffusion currents must cancel for each type of carrier:

$$J_P \text{ (drift)} + J_P \text{ (diffusion)} = 0$$

$$J_n \text{ (drift)} + J_n \text{ (diffusion)} = 0$$

Therefore, the electric field ξ builds up to the point where the net current is zero at equilibrium.
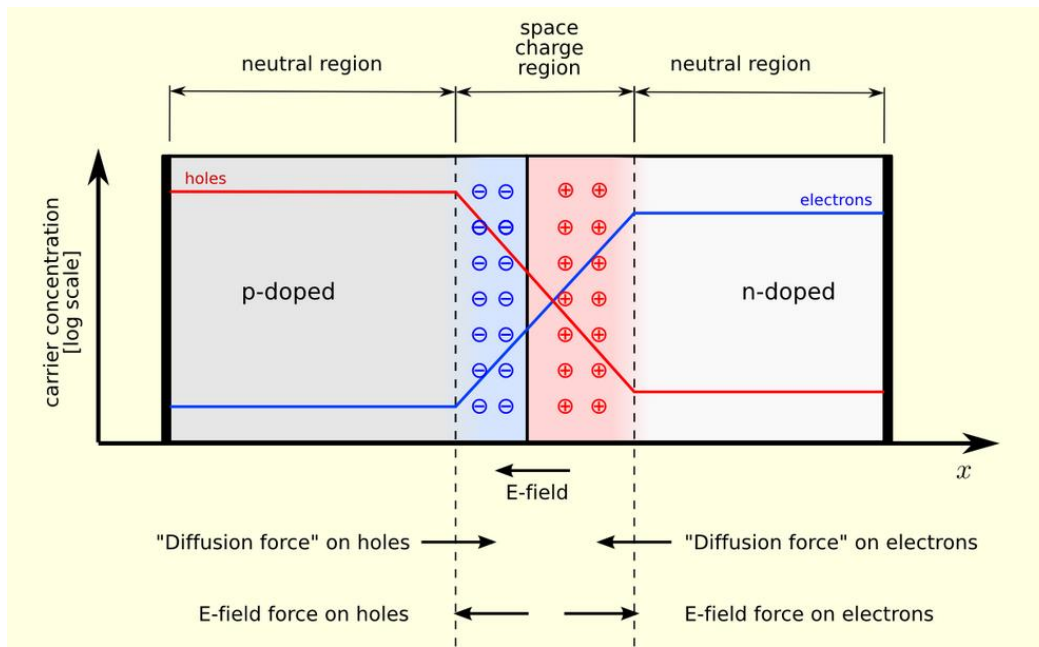
Figure 2.2: Electric field resulting from drift and diffusion currents

2.2   Principle of Operation of a Solar Cell [17]

Solar cell is a p-n junction device with no voltage directly applied across the junction. Figure 5 shows a simplified diagram of a solar cell with single p-n junction with a load.

An electric field exists in the space charge region with zero applied bias. Incident photon illumination can create electron-hole pairs in the space charge region, which are swept out of the depletion region by the built-in electric field. These swept out carriers produce photocurrent I_L in the reverse bias direction.

For simplicity, the load is assumed to be resistive. The photocurrent I_L produces a voltage drop across the resistive load which forward biases the p-n junction. This forward bias voltage produces a forward bias current, I_F. The forward bias current flows in the forward bias direction of the p-n junction. The net current, I, flowing in the reverse bias direction, is given by the equation (1).
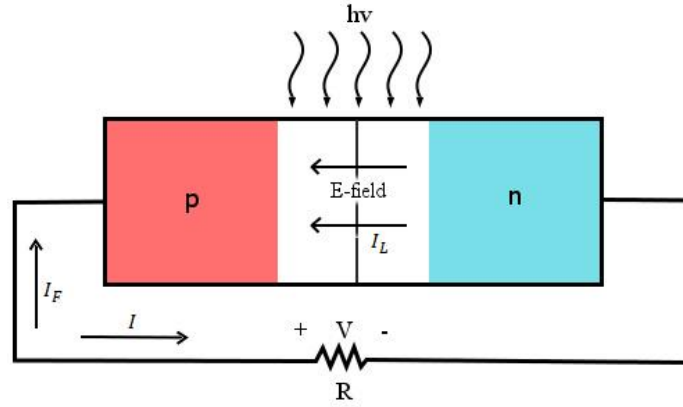
Figure 2.3: Schematic diagram of a simplified solar cell

$$I = I_L - I_F = I_L - I_S \left[\exp\left(\frac{eV}{kT}\right) - 1 \right] \qquad (1)$$

Where,

k = Boltzman constant

T = Temperature in Kelvin

q = Charge of an electron

I_s = Saturation current

2.3   Important Quantities [17]

Two important quantities used to characterize a solar cell are open-circuit voltage (V_{oc}) and short-circuit current (I_{sc}). They occur at two different limiting cases. Open circuit condition occurs when $R \rightarrow \infty$. The net current is zero and the open-circuit voltage is given by the equation (2).

$$V_{oc} = \left(\frac{kT}{q}\right) \ln\left(1 + \frac{I_L}{I_S}\right) \qquad (2)$$

The short-circuit condition occurs when R = 0. In this case V = 0 and the short-circuit current is given by the equation (3).

$$I_{sc} = I = I_L \tag{3}$$

In both open-circuit voltage and short-circuit current conditions the power output of the solar cell is zero. If P is the output power, there exists a maximum power point where $\frac{dP}{dV} = 0$ at the I-V characteristics graph. This point is called the maximum power point. The maximum output power, P_{max}, is given by,

$$P_{max} = V_{max}I_{max} \tag{4}$$

Where, V_{max} and I_{max} are voltage and current at maximum power point.

The voltage at maximum power point can be determined by differentiating the output power with respect to voltage and setting the derivative to zero. Solving for voltage iteratively from equation (5) gives V_m.

$$\left(1 + \frac{eV_{max}}{kT}\right) \exp\left(\frac{eV_m}{kT}\right) = 1 + \frac{I_L}{I_S} \tag{5}$$

The Fill factor, FF, is one of the main performance parameters of a solar cell. It is the ratio of maximum output power to the product of open-circuit voltage and short-circuit current. Fill factor can be determined by the equation (6)

$$FF = \frac{V_{max}I_{max}}{V_{oc}I_{sc}} \tag{6}$$

Efficiency of a solar cell is given by equation (7)

$$\eta = \frac{V_{oc}I_{sc}FF}{EA} \times 100\% \tag{7}$$

Where,

E = Solar irradiance (in W/cm^2)

A = Area of the surface of the solar cell (in cm^2)

The quantity I_{sc}/A can be written as J_{sc}, which is the short-circuit current density (in A/cm^2). So the equation (7) can be re-written as equation (8). This equation has been used for calculation of energy conversion efficiency.

$$\eta = \frac{V_{oc}J_{sc}FF}{E} \times 100\%$$ (8)

For terrestrial application, AM1.5G illumination condition is considered as standard illumination. In this standard, the solar irradiance, E, is taken to be 0.1 W/cm^2. For our simulation we have used AM1.5G illumination condition without concentrator. So the device is operating under single sun.

2.4 Factors Affecting Solar Cell Efficiencies

1. The actual voltage output of the module changes as lighting, temperature and load conditions change, so there is never one specific voltage at which the module operates. This reduces the overall efficiency of the solar cell [18].

2. With years of rain, hail, hot & cold cycles solar cell efficiency degrades with its age.

3. Single-junction cells have a maximum theoretical efficiency of 34% (unconcentrated light), a theoretical "infinite-junction" cell would improve this to 87% under highly concentrated sunlight [19].

4. Photons with energies lower than the band-gap energy do not get absorbed & this is known as transmission loss [20].

5. Photons with energies equal to band-gap energy Eg causes the production of an electron hole pair. When photon with energy E, greater than the band-gap energy Eg, is absorbed then the excess energy E- Eg is given off as heat to the lattice. This is known as thermalization loss [20].

6. An ideal I-V curve of a solar cell is square with fill factor (FF) = 1. But in reality the curve is exponential in nature with a maximum of FF = 0.89. This loss arises from the parasitic resistance (series and shunt resistance) of the cell. This is called fill factor loss [20].

7. Recombination losses effect both the current collection (and therefore the short-circuit current) as well as the forward bias injection current (and therefore the open-circuit voltage). This reduces the efficiency of the solar cell.

2.5   Multijunction Solar Cells [21]

The choice of materials for each sub-cell is determined by the requirements for lattice-matching, current-matching, and high performance optoelectronic properties.

For optimal growth and resulting crystal quality, the crystal lattice constant a of each material must be closely matched, resulting in lattice-matched devices. A greater degree of mismatch or other growth imperfections can lead to crystal defects causing a degradation in electronic properties.

Since each sub-cell is connected electrically in series, the same current flows through each junction. The materials are ordered with decreasing bandgaps, Eg, allowing sub-bandgap light ($\frac{hc}{\lambda} < e \times E_g$) to transmit to the lower sub-cells as shown in Fig 6, where $E_{g1} > E_{g3} > E_{g3} > E_{g4}$. Therefore, suitable bandgaps must be chosen such that the design spectrum will balance the current generation in each of the sub-cells, achieving current matching.
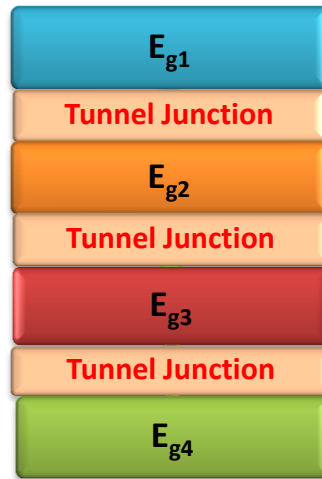
Figure 2.4: Tunnel junctions between the subcells.

Tunnel junctions are necessary since it provides a low electrical resistance connection between two subcells [22, 23]. It is usually highly doped & has a wide bandgap.

2.6   Band Grading

Band grading is a technique where by changing mole fraction the bandgap of a material can be tuned to a desired value. Several advantages can be obtained by band grading which ultimately leads to the increase in the Solar Cell efficiency.

Different materials has a range of bandgaps that can be tuned by changing the mole faction of the material e.g. AlGaAs has a bandgap range from 1.55 eV – 2.13eV [24] whereas GaInAsP has a much wider bandgap from 0.5eV – 2.1eV [25] both at 300K. With change of temperature the bandgap changes. Hence by this method a wider solar spectrum can be made available to the Solar Cell for absorption.

Theoretical analysis has shown that best results can be obtained if the energy gap gradient of the Base is not too high & the energy gap gradient of the front region is high. This is due to an

inverse window effect that occurs in the base when the energy gap gradient of the base is high [26].

A combination of graded material followed by a p-n junction could also be properly designed to increase the minority-carrier collection efficiency, through a built-in electric field. This idea was first suggested by Wolf [27] and later by Ellis and Moss [28].

Chapter 3 – The Design

3.1   Material Selection Criterion

3.1.1 Bandgap

The bandgap of a multijunction solar cell should cover a wide range in order to absorb as much of the spectrum as possible. The bandgap of each successive layer should differ by as small amount as possible, because the excess energy from light converted to heat is equal or less than the bandgap difference between photon energy and the bandgap of the absorbing material. [29].

3.1.2 Lattice Constant

It is necessary for all the layers to have similar crystal structure to produce optical transparency and maximum current conductivity in the monolithic structure. To obtain this, there should be minimum amount of lattice mismatch. The spacing of the atom locations in a crystal is described by the lattice constant. Mismatch in the crystal lattice constants of different layers creates dislocations in the lattice of the cell layers and significantly deteriorates the efficiency of the solar cell. Lattice mismatch as small as 0.01% significantly decreases the current produced by the solar cell [30].

3.1.3 Absorption Coefficient and Current Matching

It is evident from the serial architecture of monolithically grown multijunction solar cell that the output current of the solar cell is limited to the smallest of the currents produced by any of the individual junctions. So, the current through each subcell may be constrained to have the same value [30].Matching of currents in a monolithically grown multijunction solar cell is a desirable characteristic [31]. The Photocurrent is proportional to the absorption coefficient of the material and the number of incident photon that exceeds the bandgap of the material. A layer

21

must be made thinner or thicker based on its absorption coefficient and number of photons exceeding the bandgap, so that all the layers generate same photocurrent.

3.2 III – V Compounds as Photovoltaic Materials

III-V compounds have recently attracted considerable interest as elements of both single-junction and multijunction solar cells. III-V multi-junction solar cells, as a new technology which offer extremely high efficiencies compared with traditional solar cells made of a single layer of semiconductor material [32]. The special advantage that these materials offer is their wide range of variation in bandgaps [33].

Though silicon alloys are widely used, from a fundamental point of view, Si is not suitable choice for solar cell. Its bandgap is lower than the optimum bandgap required for achieving the highest level of efficiency. The optimum bandgap of the absorber should be around 1.4 eV [34] for terrestrial applications, while Si has an indirect bandgap of 1.12 eV, so not suitable for laser source. Besides this, Si has low optical absorption coefficient, compared to the high optical-absorption-compounds [35].

Photovoltaic cells fabricated from III-V compounds typically provide high output current and high efficiency. III-V ternary and quaternary alloys can offer yet more flexibility, as their bandgaps and other properties can be finely altered by changing the alloy composition.

3.3   Choice of materials
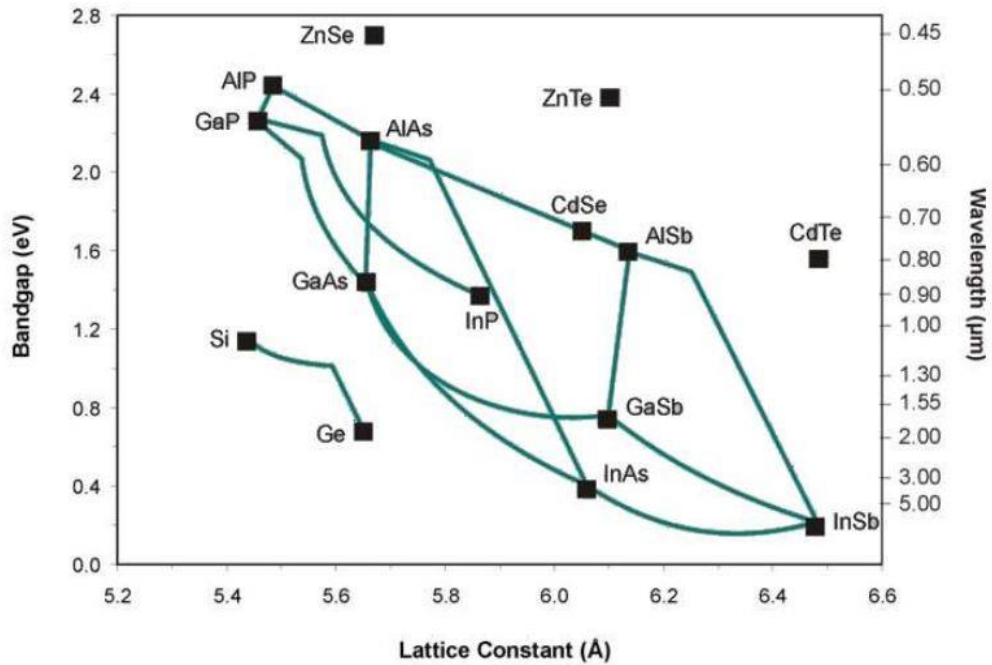
3.3.1 Choice of Layer Materials

Figure 3.1: Relation between bandgap and lattice constant of III-V ternary and quartarnery compound[36].

The figure 3.1 shows the possibility of creating a new material by combining different amount of two materials. AlAs, GaAs, Ge has roughly the same constant with different bandgaps. By combining AlAs and GaAs, the ternary compound $Al_xGa_{1-x}As$ can be made. The quaternary compound $Ga_xIn_{1-x}As_yP_{1-y}$ can be made by combining InP, GaP and GaAs. It may be possible to nearly match the lattice of $Ga_xIn_{1-x}As_yP_{1-y}$ with $Al_xGa_{1-x}As$ by changing the molar concentration i.e. changing the values of x and y (Acquisition of material properties is discussed at chapter 4). The bandgap of $Al_xGa_{1-x}As$ changes from 1.55eV to 2.13eV by varying x from 0.1 to 0.9. The bandgap of $Ga_{0.47}In_{0.53}As_yP_{1-y}$ varies from 1.27eV to 0.79eV by variation of y from 0.1 to 0.9 and keeping x constant to 0.47.

Both $Al_xGa_{1-x}As$ and $Ga_{0.47}In_{0.53}As_yP_{1-y}$ have Zinc Blende structure. The lattice constant of $Al_xGa_{1-x}As$ varies from 5.654 to 5.66 with the variation of x from 0.1 to 0.9. For $Ga_{0.47}In_{0.53}As_yP_{1-y}$ it varies from 5.69 to 5.85. So there is a lattice mismatch issue [37].

3.3.2 Choice of Substrate

Group	Material	Symbol	Bandgap (eV)	Reference
III–V	Gallium (III) Arsenide	GaAs	1.43	[15]
IV	Silicon	Si	1.11	[15]
IV	Germanium	Ge	0.67	[15]
IV–VI	Lead(II) sulfide	PbS	0.37	[15]

Table 3.1: Commonly used substrates and their bandgaps.

According to the materials selected in section 3.3.1 appropriate selection of the substrates for multiple numbers of junction are given in the following table:

Multijunction type	Substrate
1 J	GaAs
2 J	Ge

Table 3.2: Common choice of substrate for multijunction solar cell.

3.4 The Design

3.4.1 Bandgap Selection

Layer	Material	x	y	Bandgap (eV)
Window	$Al_xGa_{1-x}As$	0.8	-	2.09
Emitter	$Al_xGa_{1-x}As$	0.6	-	2.03
Base	$Al_xGa_{1-x}As$	0.5	-	2.00
BSF	$Al_xGa_{1-x}As$	0.1	-	1.55
Tunnel (n)	$Al_xGa_{1-x}As$	0.1	-	1.55
Tunnel (p)	GaAs	0	-	1.42
Window	$Ga_xIn_{1-x}As_yP_{1-y}$	0.47	0.1	1.27
Emitter	$Ga_xIn_{1-x}As_yP_{1-y}$	0.47	0.3	1.14
Base	$Ga_xIn_{1-x}As_yP_{1-y}$	0.47	0.5	1.01
BSF	$Ga_xIn_{1-x}As_yP_{1-y}$	0.47	0.8	0.84

Table 3.3: Bandgaps of $Al_xGa_{1-x}As$ and $Ga_xIn_{1-x}As_yP_{1-y}$ for selected values of x and y.

3.4.2 Layer Thickness

Layer	Thickness (μm)
Window	0.02
Emitter	0.2
Base	1
BSF	0.1
Tunnel (n)	0.01
Tunnel (p)	0.01
Window	0.03
Emitter	0.3
Base	3
BSF	0.2

Table 3.4: Thickness of different layers.

3.4.3 Doping Levels

Layer	Doping type	Doping level / cm^3
Window	P	5×10^{18}
Emitter	P	1×10^{17}
Base	N	1×10^{17}
BSF	N	1×10^{18}
Tunnel	N	1×10^{19}
Tunnel	P	1×10^{19}
Window	P	5×10^{18}
Emitter	P	1×10^{17}
Base	N	1×10^{17}
BSF	N	1×10^{18}

Table 3.5: Doping Levels of different layers

Remarks

Doping level of greater or equal to 10^{18} cm^{-3} is used in window layer [46], thus we have used the doping level of 5×10^{18}.

Typically width of the emitter is ~ 100nm [47], hence we have used emitter's of width 200nm in 1st subcell and 300nm in 2nd subcell.

In tunnel junction's usually high doping level is used [48], therefore doping level of 10^{19} was used.

Chapter - 4 Acquisitions of Material Properties

4.1   Band Structure and Carrier Concentration

4.1.1 Bandgap

The figure 4.1 shows the values of bandgap of $Al_xGa_{1-x}As$ for different value of x in the range 0.1 to 0.9 [38].

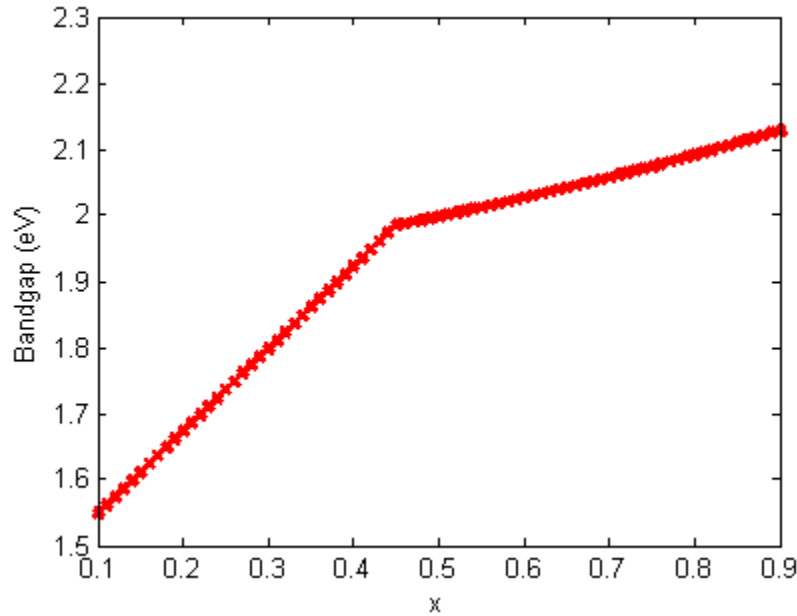Figure 4.1: Bandgap vs. x for $Al_xGa_{1-x}As$.

According to the material selection criterion, bandgap should be in a decreasing order from top to bottom. The chosen values of bandgap for $Al_xGa_{1-x}As$ in this work and the corresponding values of x are tabulated in table 4.1.

Name of Layer (Top Cell)	X	Bandgap (eV)
Window	0.8	2.09
Emitter	0.6	2.03
Base	0.5	1.99
BSF	0.1	1.55

Table 4.1: Values of bandgap for selected values of x of $Al_xGa_{1-x}As$.

The figure 4.2 shows the values of bandgap of $Ga_{0.47}In_{0.53}As_yP_{1-y}$ for different value of y in the range 0.1 to 0.9 [39].
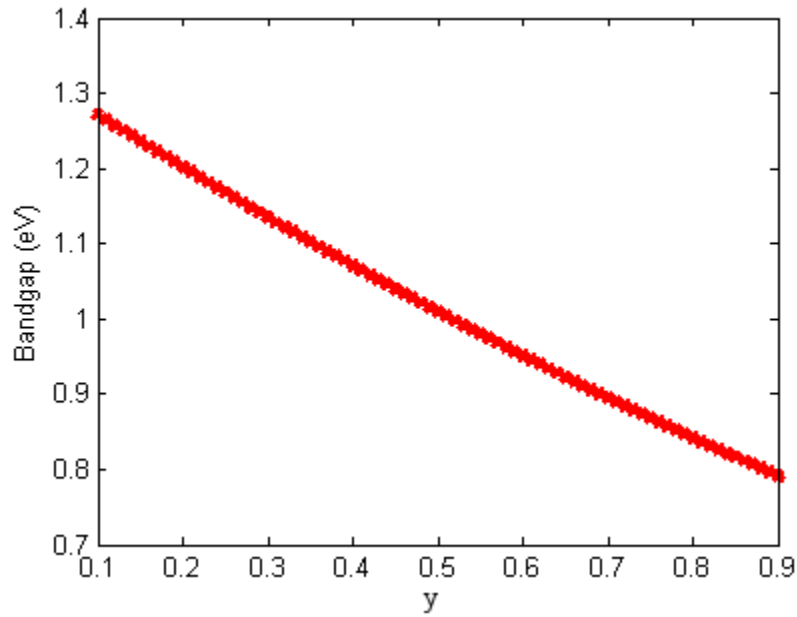

Figure 4.2: Bandgap vs. y for $Ga_{0.47}In_{0.53}As_yP_{1-y}$.

The chosen values of bandgap for $Ga_{0.47}In_{0.53}As_yP_{1-y}$ in this work and the corresponding values of y are tabulated in table 4.2.

Name of Layer (Bottom Cell)	Y	Bandgap (eV)
Window	0.1	1.27
Emitter	0.3	1.14
Base	0.5	1.01
BSF	0.8	0.84

Table 4.2: Values of bandgap for selected values of y of $Ga_{0.47}In_{0.53}As_yP_{1-y}$.

4.1.2 Carrier Concentration
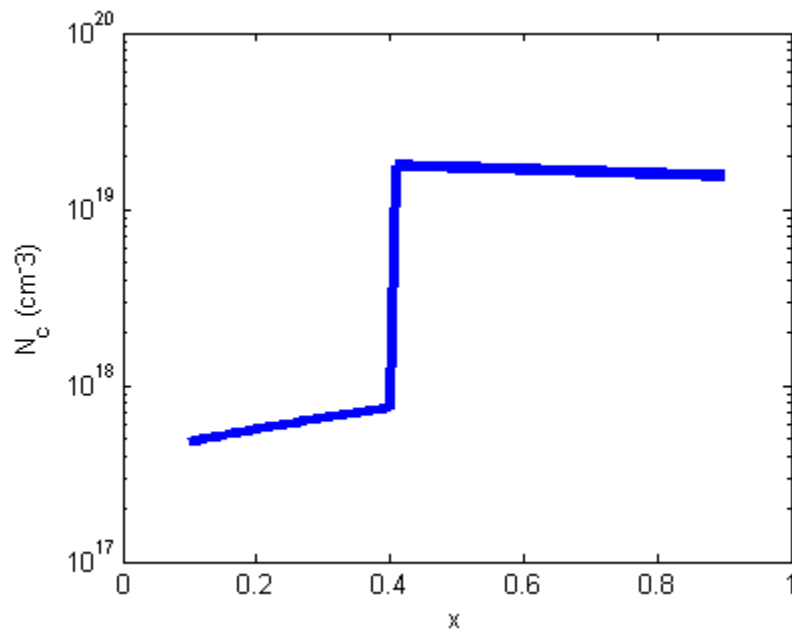

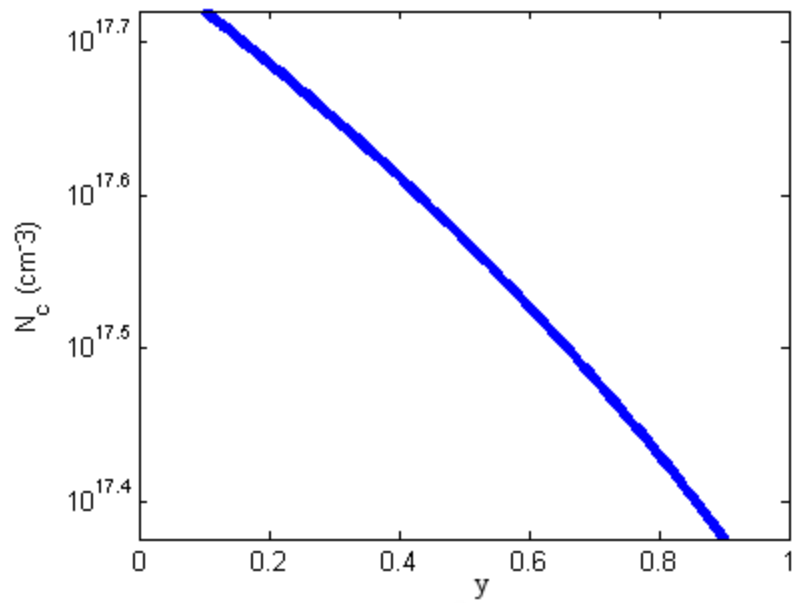Figure 4.3: Effective conduction band density of states for $Al_xGa_{1-x}As$ vs. x [38].

Figure 4.4: Effective conduction band density of states for $Ga_{0.47}In_{0.53}As_yP_{1-y}$ vs. y [39].

4.2   Electrical Properties

4.2.1 Mobility Parameters

$Ga_{0.47}In_{0.53}As_yP_{1-y}$:
Electron mobility [41, 42].
Hole mobility [41].

$Al_xGa_{1-x}As$:
Electron mobility [43, 44].
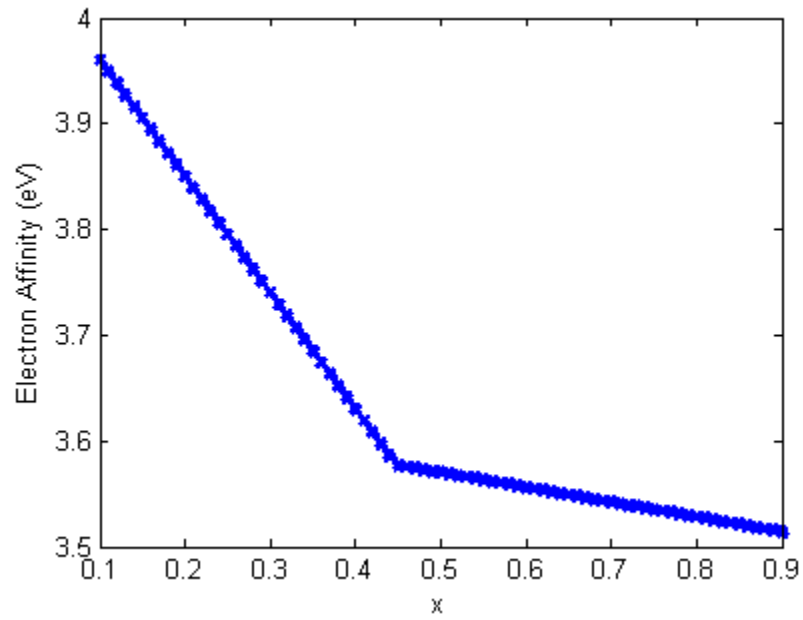Hole mobility [44, 45].

4.2.2 Electron Affinity

Figure 4.5: Electron affinity for $Al_xGa_{1-x}As$ vs. x [38].
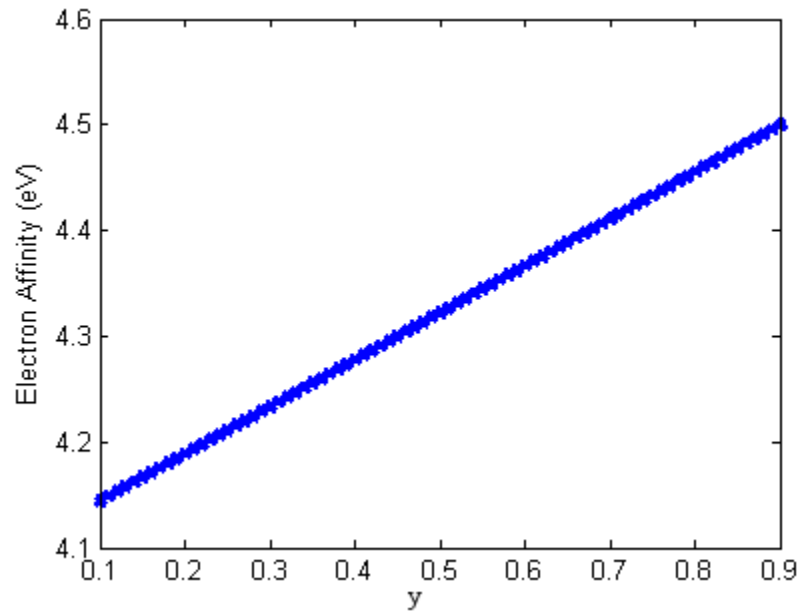
Figure 4.6: Electron affinity for $Ga_{0.47}In_{0.53}As_yP_{1-y}$ vs. y [39].

4.3 Optical Properties

4.3.1 Absorption Coefficient
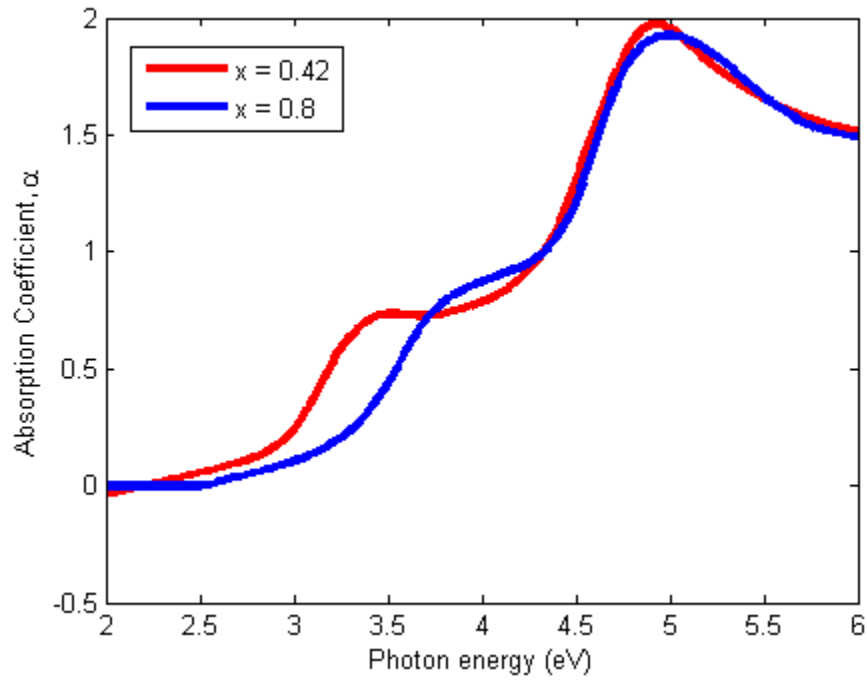
Figure 4.7: Absorption coefficient for $Al_xGa_{1-x}As$ [40].
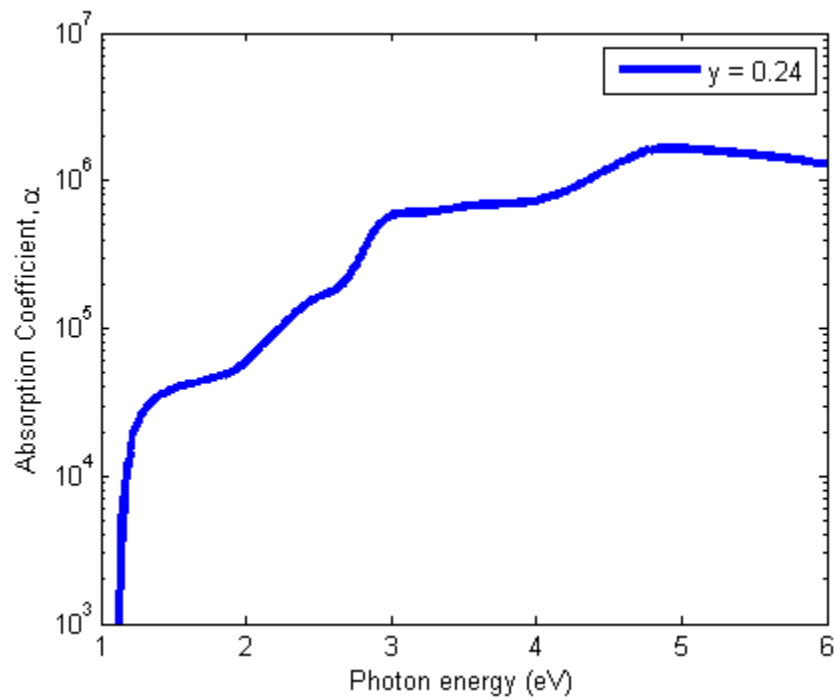
Figure 4.8: Absorption coefficient for $Ga_{0.47}In_{0.53}As_yP_{1-y}$ [39].

Remarks

To obtain unknown data's we have used interpolation or linearly divided the spacing between the data available, from the references, for two consecutive mole fractions to obtain accurate data for any intermediate mole fraction. Data for our desired mole fractions were obtained and are depicted in Figure 4.1 to 4.8.

Chapter - 5 Simulation & Results

5.1   Results

Using the materials chosen in chapter 3 we have developed a 2-Junction Solar cell shown in the following figure:

$Al_{0.8}Ga_{0.2}As$	p	Window
$Al_{0.6}Ga_{0.4}As$	p	Emitter
$Al_{0.5}Ga_{0.5}As$	n	Base
$Al_{0.1}Ga_{0.9}As$	n	BSF
$Al_{0.1}Ga_{0.9}As$	n	Tunnel
GaAs	p	Tunnel
$Ga_{0.47}In_{0.53}As_{0.1}P_{0.9}$	p	Window
$Ga_{0.47}In_{0.53}As_{0.3}P_{0.6}$	p	Emitter
$Ga_{0.47}In_{0.53}As_{0.5}P_{0.5}$	n	Base
$Ga_{0.47}In_{0.53}As_{0.8}P_{0.2}$	n	BSF
Ge	n	Substrate

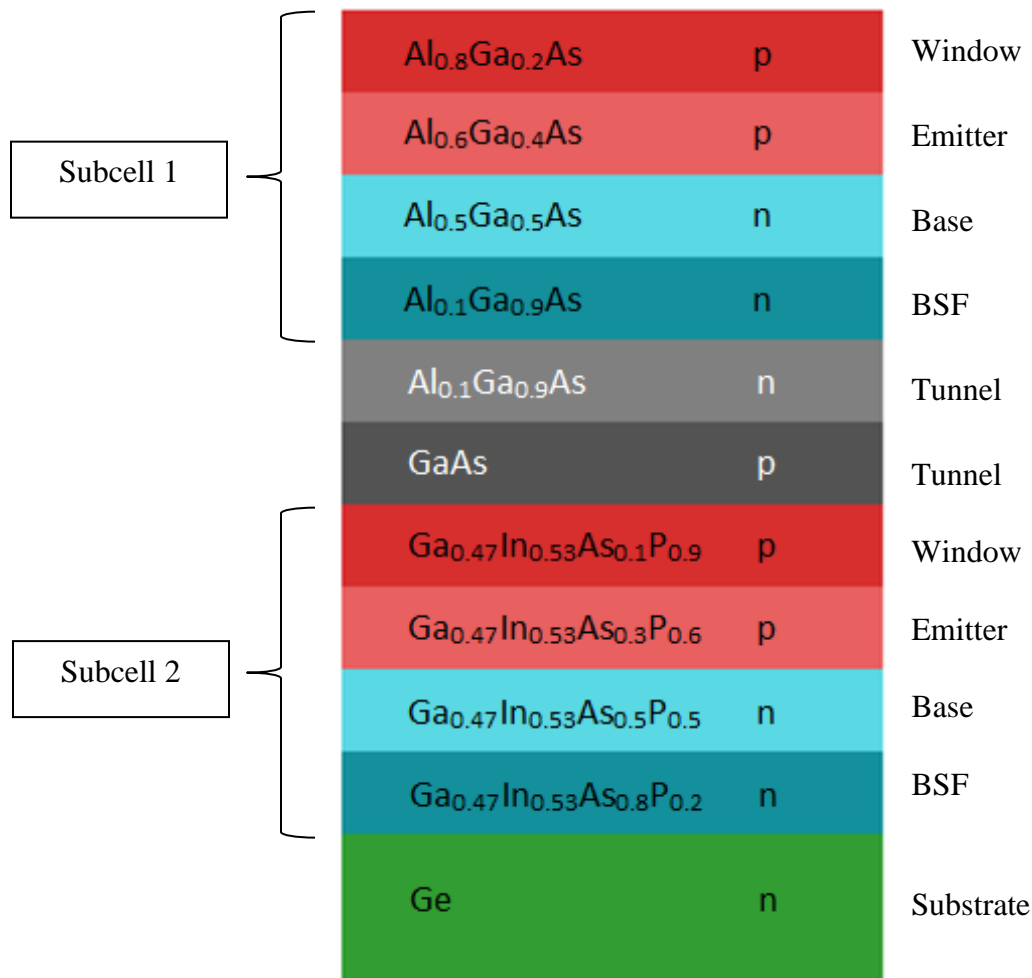Subcell 1 (layers 1–4), Subcell 2 (layers 7–10)

Figure 5.1: Diagram of designed 2-Junction Solar cell

From the data in Chapter 4 we have used AMPS1D & wxAMPS to obtain the I-V characteristic curve, shown in figure 5.2, of the designed Solar cell. Using the software short circuit current

density (Jsc), open circuit voltage (Voc), Fill Factor (FF) & Solar cell efficiency were also calculated.

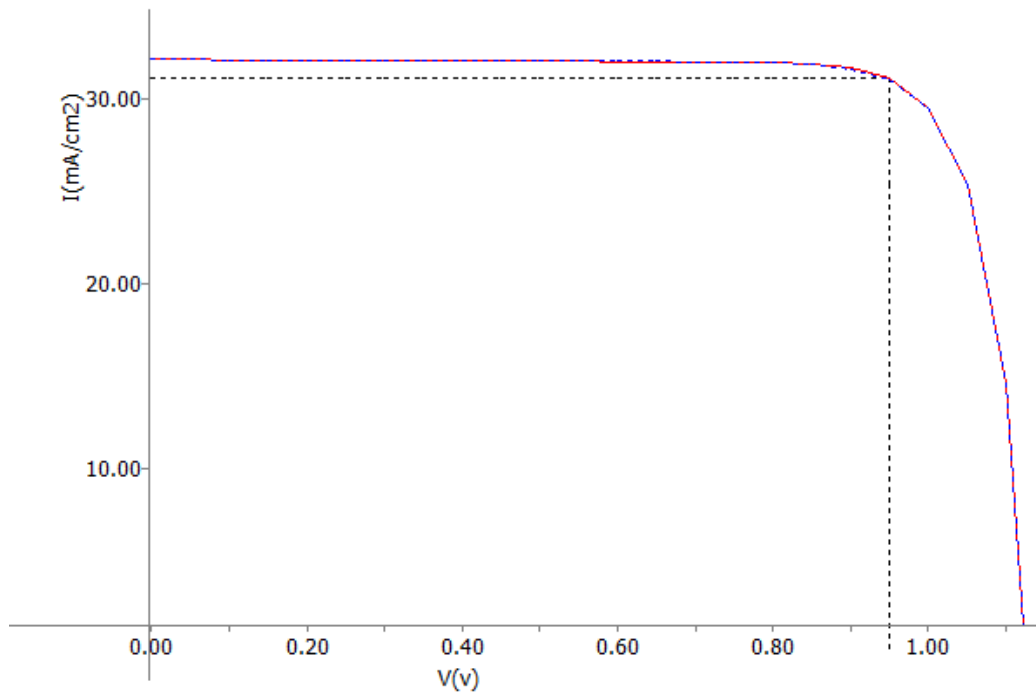Figure 5.2: I-V characteristic curve of the designed 2-Junction Solar cell

Results:

Open circuit voltage, Voc = 1.262 V

Short circuit current density, Jsc = 32.1187 mA/cm^2

Fill Factor, FF = 81.691 %

Efficiency, η = 29.55 %

5.2   Tunnel junction optimization

The tunnel junction was made from $Al_xGa_{1-x}As$ of n & p type. By varying the mole fraction x, different bandgap combinations of the n type & the p type materials, of the tunnel junction, were applied and the respective results were obtained. The n type material of the tunnel junction was given the bandgap of 1.55 eV while the bandgap of p type material was changed from 1.424 eV [15] (for x = 0, i.e. GaAs) to 1.55 eV [24] (for x = 0.1) & the corresponding Solar cell efficiency was calculated. The variation of the Solar cell efficiency with the change in bandgap is shown in the figure below:
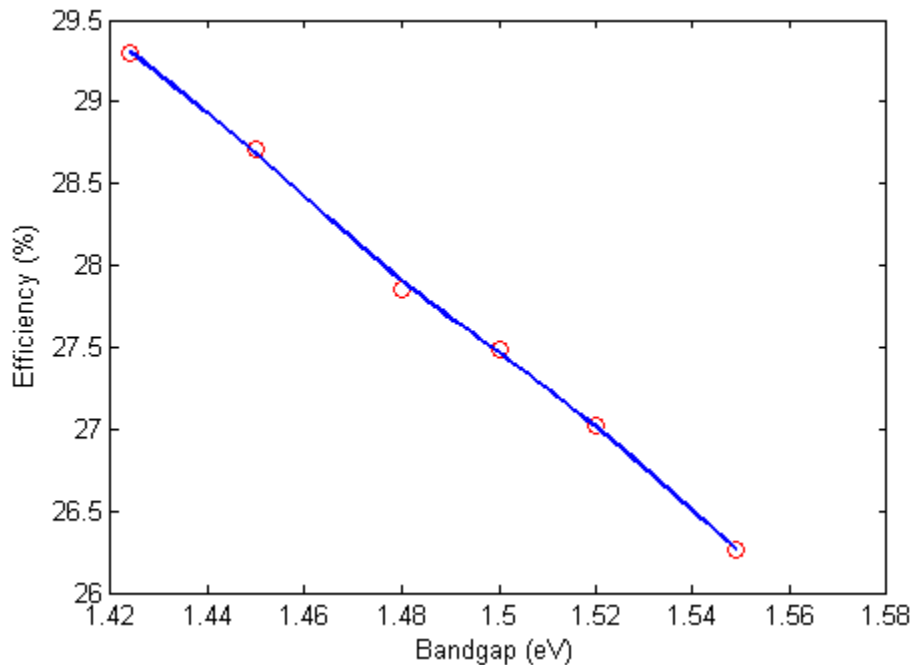
Figure 5.3: Variation of efficiency with the change of bandgap of p-type material of the tunnel junction

From the above figure it is found that a larger bandgap difference between the n & p type material of the tunnel junction provides lower resistance connection between subcells hence produces a higher efficiency of the Solar cell. Hence for the p type material of the tunnel junction we have used the mole fraction x=0, which gives the bandgap that of GaAs (1.424 eV), thus obtaining a higher bandgap difference of (1.55 eV - 1.42 eV) 0.13 eV between the n & p type material of the tunnel junction & correspondingly achieving a higher efficiency.

Chapter - 6 Summary

6.1 Conclusions

Multijunction Solar cell of two subcells was developed using $Al_xGa_{1-x}As$ in the 1st subcell & GaInAsP in the 2nd subcell. The whole structure is to be grown on Ge subcell since the BSF layer of the 2nd subcell had a bandgap of 0.84 eV. By choosing appropriate values of the mole fractions suitable bandgap were used in the descending order to design the whole cell. Finally tunnel junction was optimized and an overall cell efficiency of 29.55% with a Fill Factor of 81.691% was obtained.

6.2 Future Work

For further optimization of this design we would like to apply bandgrading technique and optimize each of the layers.

We would also like to extend this design for 2 Junction to make 3 & 4 Junctions. A design for 3-Junction & 4-Junction is proposed and are shown in Figure 6.1 and Figure 6.2 respectively.

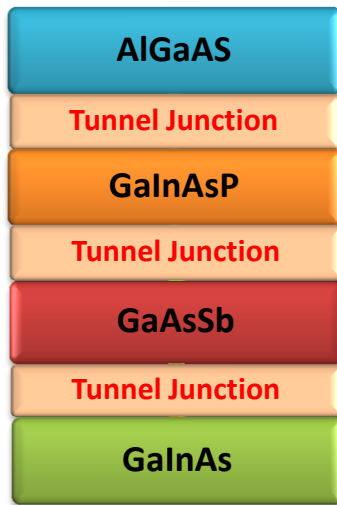Figure 6.1: Design proposal for 3-Junction Solar cell

Figure 6.2: Design proposal for 4-Junction Solar cell

Bibliography

1. Zehner, Ozzie (2012). *Green Illusions*. Lincoln and London: University of Nebraska Press. pp. 1–169, 331–42.

2. Perlin, John (2004). "The Silicon Solar Cell Turns 50". National Renewable Energy Laboratory. Retrieved 5 October 2010.

3. Chetan Singh Solanki. Renewable Energy Technologies. Prentice Hall India.

4. S.Sivanaguruji; M.Balasubba Reddy, D.Srilatha. Generation and Utilization of Electrical Energy, Pearson

5. Chetan Singh Solanki. Renewable Energy Technologies. Prentice Hall India.

6. SolidWorks Plays Key Role in Cambridge Eco Race Effort. cambridgenetwork.co.uk (4 February 2009).

7. "The ODOT Solar Highway". Oregon Dept. of Transportation. Retrieved 22 April 2011.

8. Semiconductor Physics And Devices, Donald A. Neamen.

9. Lenardic, Denis. Large-scale photovoltaic power plants ranking $1 - 50 PVresources.com$.

10. Ariel, Yotam (25 August 2011) Delivering Solar to a Distribution-cursed Market. Renewableenergyworld.com. Retrieved on 3 June 2012.

11. "Solar on cheap", physics.ucsc.edu. Retrieved 2011-06-30.

12. John R. Balfour. Introduction to Photovoltaics. Jones & Bartlett Learning.

13. AMPS-1D User Manual.

14. AMPS-1D User Manual.

15. Streetman, Ben G.; Sanjay Banerjee. *Solid State electronic Devices* (6th ed.).New Jersey: Prentice Hall.

16. M. Wolf, Proc. IRE 48, 1246 (I 960).

17. Semiconductor Physics And Devices, Donald A. Neamen.

18. Chetan Singh Solanki. Renewable Energy Technologies. Prentice Hall India.

19. F. Dimroth, 3-6 junction photovoltaic cells for space and terrestrial applications, Photovoltaic Specialists Conference, 2005.

20. Chetan Singh Solanki, Solar Photovoltaics : Fundamentals, Technologies and Applications.

21. Nikhil Jain, Design of iii-v Multijunction Solar Cells on Silicon Substrate .

22. Yamaguchi, M; Takamoto, T; Araki, K (2006). "Super high-efficiency multi-junction and concentrator solar cells". *Solar Energy Materials and Solar Cells* **90** (18–19): 3068.doi:10.1016/j.solmat.2006.06.028.

23. Low resistance tunnel junctions for high efficiency tandem solar cells, EP 2135290 A2

24. GaAs, AlAs, and $Al_xGa_{1-x}As$ Material parameters for use in research and device applications, Sadao Adachi, J. Appl. Phys. 58, R1 (1985); doi: 10.1063/1.336070.

25. A.T. Gorelenok, A.G. Dzigasov, P.P. Moskvin, V.S. Sorokin, I.S. Tarasov, Sov. Phys.Semicond., 15, no.12, pp.1400-1402 (1981).

26. Theoretical analysis of solar cells based on graded bandgap structures, By: G. Sassi Citation: J. Appl. Phys. 54, 5421 (1983); doi: 10.1063/1.332723.

27. M. Wolf, Proc. IRE 48, 1246 (I 960).

28. B. Ellis and T.S. Moss, Solid-State Electron. 13,1 (1970).

29. K. Zweibel, Basic photovoltaic principles and methods, New York: Van Nostrand Reinhold, 1984.

30. B. Burnett, The basic physics and design of III-V multijunction solar cells, 2002.

31. G. P. Smestad, Optoelectronics of solar cells,Bellingham, WA: SPIE Press, 2002.

32. Luque, A., Martı´, A., Stanley, C., Lo´pez, N., Cuadra, L., Zhou, D., & Mc Kee, A. (2004). General equivalent circuit for intermediate band devices: Potentials, currents and electroluminescence. J. Appl. Phys., 96(03), 903-909.

33. J.E. Sutherland, and J.R. Hauser, "Optimum bandgap of several III–V heterojunction solar cells", Solid-State Electronics, vol. 22, no. 1, pp. 3-5, 1979.

34. T. Tiedje, E. Yablonovitch, G. D. Cody, and B. G. Brooks, "Limiting efficiency of Silicon solar cells", IEEE Transactions on Electron Devices, vol. ED-31, pp. 711-716, 1984.

35. L.W. James, "III-V Compound heterojunction solar cells", in Proceedings of IEEE International Electron Devices Meeting, vol. 21, pp. 87-90, Washington, USA, 1975.

36. J. M. Román, State-of-the-art of III-V solar cell fabrication technologies, device designs and applications, Advanced Photovoltaic Cell Design, 2004.

37. Material parameters of InGaAsP and related binariesS Adachi - Journal of Applied Physics, 1982][GaAs, AlAs, and Al_xGa_{1-x}As Material parameters for use in research and device applications.

38. GaAs, AlAs, and Al_xGa_{1-x}As Material parameters for use in research and device applications, Sadao Adachi, J. Appl. Phys. 58, R1 (1985); doi: 10.1063/1.336070.

39. Goldberg Yu.A. and N.M. Schmidt *Handbook Series on Semiconductor Parameters*, **vol.2**, M. Levinshtein, S. Rumyantsev and M. Shur, ed., World Scientific, London, 1999, pp. 153-179.

40. Goldberg Yu.A. Handbook Series on Semiconductor Parameters, vol.2, M. Levinshtein, S. Rumyantsev and M. Shur, ed., World Scientific, London, 1999, pp. 1-36.

41. T.P.Pearsall, *GaInAsP Alloy Semiconductors*, John Wiley and Sons, 1982.

42. K.Tappura, *J. Appl. Phys.*, **74**, no. 7, pp.4565-4570 (1993).

43. A.K.Saxena, Phys. Rev., B24, no.6, pp. 3295-3302 (1981).

44. M.Shur, Physics of Semiconductor Devices, Prentice Hall, 1990.

45. W.C.Liu, *J. Material Sci.*, **25**, no.3, pp.1765-1772 (1990).

46. Luque, Antonio; Hegedus, eds. (2003). Handbook of Photovoltaic Science and Engineering. John Wiley and Sons. ISBN 0-471-49196-9.

47. Computer modeling study of the effects of inhomogeneous doping and/or composition in GaAs solarcell devices H. C. Hamaker, J. Appl. Phys. 58, 2344 (1985); doi: 10.1063/1.335957.

48. Tunnel-Junction-Limited Multijunction Solar Cell Performance Over Concentration; doi: 10.1109/JSTQE.2013.2258140.

49. J. A. Hutchby and R. L. Fudrich "Theoreti cal anal ysi s of AlxGa1-xAs/GaAs graded band gap solar cell " J. Appl . Phys. 47, pp.3140-3151 1976.